Synthesis and evaluation of hydrogen peroxide sensitive tofacitinib prodrugs

Previtali, Viola; Keiding, Ulrik Bering; Olsen, Asger Hegelund; Peiró Cadahía, Jorge; Clausen, Anne Skovsbo; Kjaer, Andreas; Andresen, Thomas Lars; Hansen, Anders Elias; Clausen, Mads Hartvig

Published in:
European Journal of Medicinal Chemistry Reports

Link to article, DOI:
10.1016/j.ejmcr.2021.100019

Publication date:
2022

Document Version
Publisher's PDF, also known as Version of record

European Journal of Medicinal Chemistry Reports 4 (2022) 100019

HOSTED BY

Contents lists available at ScienceDirect

European Journal of Medicinal Chemistry Reports

journal homepage: www.editorialmanager.com/ejmcr/default.aspx

Synthesis and evaluation of hydrogen peroxide sensitive tofacitinib prodrugs

Viola Previtali [a,b], Ulrik Bering Keiding [a,b], Asger Hegelund Olsen [a,b], Jorge Peiró Cadahía [a,b], Anne Skovsbo Clausen [c,d], Andreas Kjaer [c,d], Thomas Lars Andresen [a,e], Anders Elias Hansen [a,e], Mads Hartvig Clausen [a,b,*]

[a] Center for Nanomedicine & Theranostics, Technical University of Denmark, Denmark
[b] Department of Chemistry, Technical University of Denmark, Kemitorvet 207, 2800, Kgs. Lyngby, Denmark
[c] Cluster for Molecular Imaging, Department of Biomedical Sciences, University of Copenhagen, Blegdamsvej 3, 2200, Copenhagen, Denmark
[d] Department of Clinical Physiology, Nuclear Medicine & PET, Rigshospitalet, Blegdamsvej 9, 2100, Copenhagen, Denmark
[e] Biotherapeutic Engineering and Drug Targeting, Department of Health Technology, Technical University of Denmark, Produktionstorvet, 2800, Kgs. Lyngby, Denmark

ARTICLE INFO

Keywords:
Rheumatoid arthritis
Inflammation
Tofacitinib
Prodrug
Janus kinase inhibitor
Reactive oxygen species

ABSTRACT

Tofacitinib (CP-690,550), an approved Janus kinase (JAK) inhibitor, has been proven highly efficacious in treating rheumatoid arthritis (RA). Unfortunately, tofacitinib's clinical application has been limited by adverse side effects that arise from its pan-JAKs inhibition and ubiquitous biodistribution. In this study, we have examined whether a reactive oxygen species (ROS)-activated prodrug design could be applied to tofacitinib to potentially avoid its systemic JAK inhibition and thereby reduce its adverse effects. The prodrug strategy selected is based on ROS-labile 4-methylphenylboronic acid pro-moieties linked to the drugs via a carbamate linkage (prodrug **1**) or a direct C–N bond (prodrug **2**). Activation under pathophysiological concentrations of H_2O_2 was investigated and conversion to desired tofacitinib assessed. The most promising prodrug candidate, prodrug **2**, was selected in agreement with relevant *in vitro* physicochemical assay and *in silico* predicted ADME properties. Selected candidate prodrug **2** showed a remarkable potency window compared to tofacitinib in an *in vitro* kinase assay against JAK1 and JAK3 kinases. Importantly, prodrug **2** displayed a similar pharmacokinetic profile to tofacitinib after single dose *i.p.* administration to DBA/1 mice. This study supports the promising applications of ROS-sensitive tofacitinib prodrugs. Their further development and applicability would enhance tofacitinib's therapeutic efficacy, and may provide an opportunity for future development of safer tofacitinib dosing regimens.

1. Introduction

Tofacitinib (CP-690,550) is a JAK (Janus kinase) inhibitor approved by the US Food and Drug Administration (FDA) in 2012 for the treatment of adults with moderate-to-severe rheumatoid arthritis (RA). It was the first drug targeting a specific protein kinase to be developed outside the field of cancer [1]. Tofacitinib has also been used successfully for psoriatic arthritis, ulcerative colitis, and, in the last year, in trials to test its effect in lowering the risk of death and respiratory failure among patients hospitalized with Covid-19 pneumomnia [2].

The success of tofacitinib stimulated the development of additional JAK inhibitors, which are either already approved (e.g. baricitinib, upadacitinib, and filgotinib) or undergoing clinical trials for others immune-mediated diseases beyond rheumatoid arthritis [3–5].

Tofacitinib is a pan-JAK kinase inhibitor that targets four members of the JAK family of protein tyrosine kinases, JAK1, JAK2, JAK3, and TYK2 [6], modulating the actions of about 25 cytokines and interferons [1]. Despite the indisputable advantages of using tofacitinib for patients who do not respond, or are intolerant to methotrexate [7],

Abbreviations: ADME, absorption, distribution, metabolism, excretion; ATP, adenosine triphosphate; AUC, area under curve; DBA, dilute brown non-agouti; DIPEA, *N,N*-diisopropylethylamine; DMF, dimethylformamide; FDA, US Food and Drug Administration; i.p., intraperitoneal; JAK, Janus kinase; PAINS, pan-assay interference compounds; PBS, phosphate buffered saline; RA, rheumatoid arthritis; ROS, reactive oxygen species.

* Corresponding author. Center for Nanomedicine & Theranostics, Technical University of Denmark, Kemitorvet 207, 2800 Kgs. Lyngby, Denmark.
E-mail address: mhc@kemi.dtu.dk (M.H. Clausen).

https://doi.org/10.1016/j.ejmcr.2021.100019
Received 16 October 2021; Received in revised form 17 November 2021; Accepted 20 November 2021
Available online 24 November 2021

tofacitinib's multi-target activity is also responsible for its undesirable side effects, including infection, lipid levels alterations, and malignancies [8].

The long history of safety concerns is a serious impediment that affects JAK inhibitors other than tofacitinib, casting doubt on their long-term use for rheumatoid arthritis treatment [9]. In this perspective, newer and selective JAK inhibitors that narrow the spectrum of cytokine pathways involved are now under development, but, despite the hypothesis that improved JAK selectivity is possible and efficacious against inflammatory diseases, clinical approval is still pending [10].

Other than the development of JAK-selective inhibitors, one way of potentially reducing adverse effects is to avoid systemic JAK inhibition, given that tofacitinib's toxicity can in part be attributed to its ubiquitous biodistribution [11].

In this context, a number of reactive oxygen species (ROS)-sensitive functionalities have been identified for introducing disease-targeting properties into small molecule drugs – a prodrug strategy that offers a promising approach for increasing the selectivity and efficacy of treatments [12–14]. Applications of ROS sensitive prodrugs encompass many therapeutic areas, among the latest we find: gemcitabine derivatives for the selective treatment of pancreatic ductal adenocarcinoma [15], Keap1-Nrf2 targeting prodrugs for selective activation in inflammatory conditions [16], a selective small molecule ATF6 activator for protection of tissue damage following ischemia/reperfusion [17], and first in class tyrosine kinase inhibitor crizotinib prodrug [1].

Examples of ROS sensitive prodrugs using JAK inhibitors and application in RA was recently presented by Bao et al. with their report of an H_2O_2-inducible JAK3 covalent inhibitor [18]. Moreover, in 2018 Wei et al. reported the development of a macromolecular prodrug of tofacitinib with modified pharmacokinetics and biodistribution properties, favoring accumulation in arthritic joints and reducing systemic JAK inhibition [19].

Inspired by the ROS-activated prodrug strategy and following our previous work [20,21], we designed and synthesized prodrugs **1** and **2**. The compounds both have a ROS-labile 4-methylphenylboronic acid promoiety linked to the tofacitinib pyrrolopyrimidine via a carbamate linkage (**1**) or a direct C–N bond (**2**, Fig. 1). Triggered by ROS (e.g. hydrogen peroxide, H_2O_2) the B–C bond undergoes oxidation via coordination of H_2O_2 to the boron atom followed by aryl bond migration to form an intermediate borate that rapidly hydrolyses in water to generate a phenol and boric acid (Fig. 1). To assess the ability of prodrugs **1** and **2** to release tofacitinib, we evaluated their activation profile. Chemical stability was also investigated and compared with negative control **3** that is lacking the boronic acid. Furthermore, physicochemical properties and *in silico* descriptors to predict ADME parameters and drug-likeness of the prodrugs were evaluated. Additionally, *in vitro* JAK1/JAK3 kinase inhibition of the prodrugs was assessed, and the *in vivo* pharmacokinetics evaluated to compare them to the parent drug tofacitinib.

2. Results and discussion

2.1. Synthesis of prodrugs

Tofacitinib was purchased as its citrate salt and used as a starting point for synthesis of prodrugs **1**, **2**, and negative control **3**. Pinacolate **4** was converted into the corresponding chloroformate **5** with phosgene, as previously described [20]. Coupling between tofacitinib citrate and **5** afforded pinacol-intermediate **6**, which underwent oxidative cleavage with sodium periodate to deliver prodrug **1** in a good yield. Similarly, coupling between tofacitinib citrate and benzyl chloroformate **7** afforded compound **3**, used as a negative control due its lacking of the ROS-liable boron-containing moiety. Alkylation of tofacitinb citrate with 4-(bromomethyl)phenyl)boronic acid **8** afforded the second prodrug, **2** (Scheme 1).

2.2. Activation of prodrugs

H_2O_2 is the most stable ROS and, under pathological inflammatory conditions, its extracellular concentration can be as high as 1.0 mM [12]. We therefore moved to the investigation of the effect of H_2O_2 on prodrug activation. We evaluated the release of prodrug **1** and **2** using H_2O_2 at different concentrations (0.25 mM and 1 mM) for up to 24 h and at 37 °C. As shown in Fig. 2(A), prodrug **1** was completely converted to tofacitinib

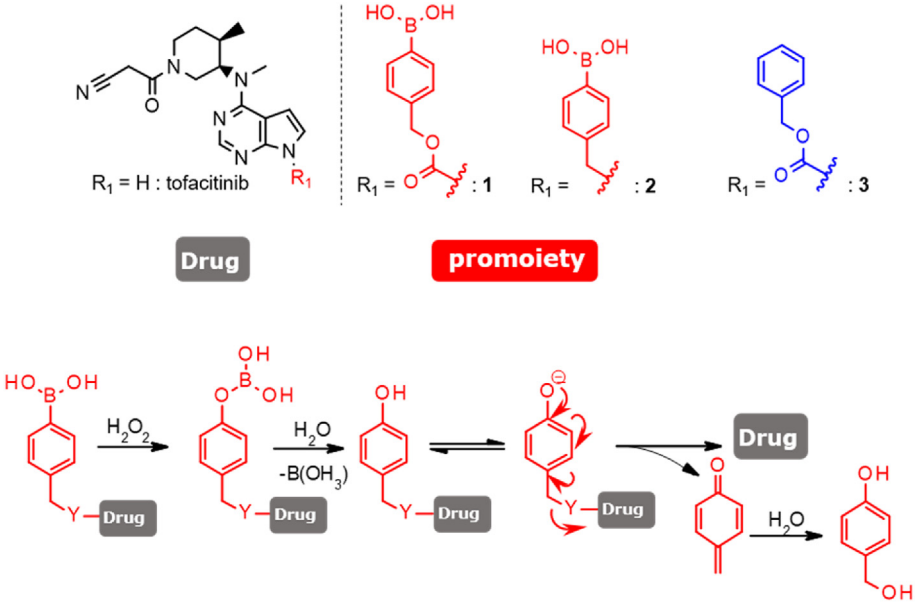

Fig. 1. Structures of tofacitinib, proposed prodrugs **1** and **2**, negative control **3**, and their H_2O_2-mediated release mechanism.

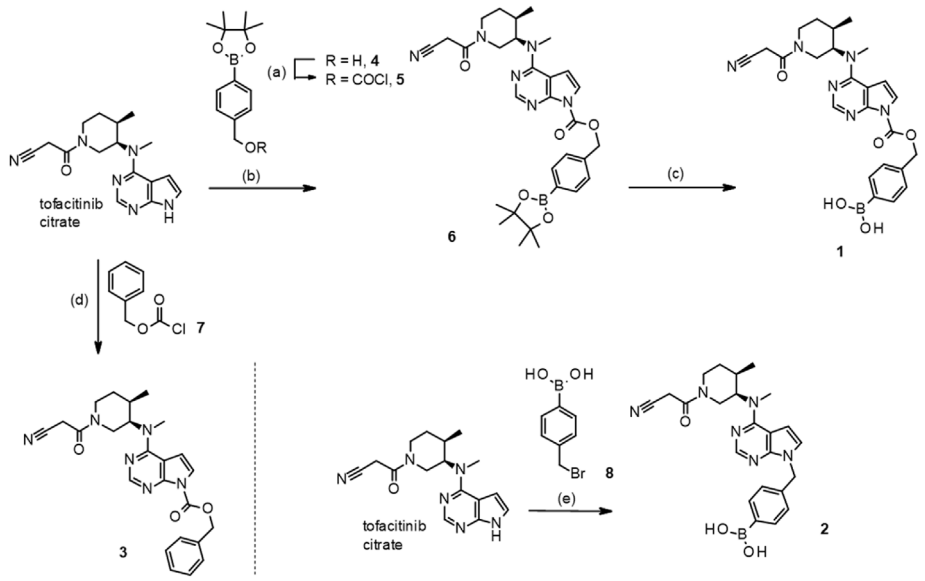

Scheme 1. Synthesis of tofacitinib prodrugs **1** and **2**, and negative control **3**[a].
[a]Reagents and conditions: (a) phosgene (20% in toluene), dioxane, rt, 16 h, 100% [20]; (b) **5**, DIPEA, CH_2Cl_2, 0 °C, 4 h, 20%; (c) acetone, $NaIO_4$, NH_4OAc (aq., 500 mM), rt, 2 h, 70%; (d) CbzCl **7**, DIPEA, CH_2Cl_2, 0 °C to rt, 16 h, 54%; (e) 4-(bromomethyl)phenyl)boronic acid **8**, DIPEA, DMF, 55 °C, 2 h, 27%.

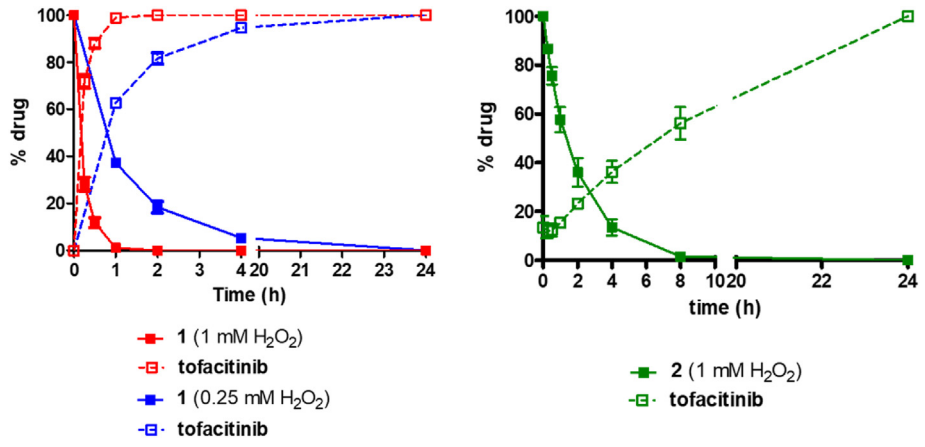

Fig. 2. Activation profile of prodrugs **1** (A, left) and **2** (B, right).

after only 1 h of incubation with H_2O_2 at 1 mM, while using H_2O_2 at 0.25 mM, complete conversion was achieved at 24 h. Comparatively, complete conversion of prodrug **2** was achieved after 8 h of incubation with H_2O_2 at 1 mM. As expected, the release of tofaticinib was significantly slower due to the metastable intermediate phenol, and was only achieved after ≥24 h Fig. 2(B). This behavior is in line with previous observations for prodrugs of MTX and AMT having a carbamate and C–N linker, respectively [20]. Importantly, the AMT prodrug was active in a CIA mouse model of arthritis, demonstrating that longer release times does not hamper activity of the parent drug upon release.

Table 1
Chemical stability and permeabilityof **tofacitinib** free base, **1**, and **3**.

	Tofacitinib (free base)	1	3
PBS ($t_{½}$, h)	–	>24	–
SGF	–	23.7 ± 3.1	>24
SIF	–	0.7 ± 0.1	<1
PAMPA (Pe, × 10^{-6} cm/s)	0.82 ± 0.11	BQL	–

SGF: simulated gastric fluid; SIF: simulated intestinal fluid; PAMPA: parallel artificial membrane permeability assay.

2.3. Chemical stability and physicochemical properties

We then moved to the evaluation of the chemical stability and permeability, see Table 1. Predicted adsorption, distribution, metabolism, excretion (ADME) parameters of prodrug **1**, prodrug **2**, and the parent drug tofacitinib were calculated using the web tool SwissADME [22], and can be found in supporting information.

The carbamate linker common to prodrug **1** and negative control **3** was stable in PBS and simulated gastric fluid (SGF) with half-lives above 24 h. In simulated intestinal fluid (SIF), the half-life for prodrug **1** was found to be lower than 1 h, indicating a chemical liability traceable to the carbamate linker rather than the *C*–B bond, since the half-life of negative control **3** was also highly reduced (<1h, Table 1).

Predicted solubility for prodrugs **1** and **2** was 56.8 μg/mL and 87.0 μg/mL respectively, against a higher solubility of 559 μg/mL for tofacitinib (Table S1).

Overall, despite the good ROS-activation profile and no PAINS alerts, prodrug **1** proved to be unstable in SIF and has low solubility that prevented further investigation. Instead, we decided to investigate prodrug **2** further in an *in vitro* JAK inhibition assay and to evaluate its *in vivo* pharmacokinetics compared to tofacitinib.

2.4. In vitro kinase assay

Tofacitinib is a reversible, competitive inhibitor that binds to the adenosine triphosphate (ATP) binding site and, as a result, inhibits the phosphorylation and activation of the JAK family of kinases. This prevents the phosphorylation and activation of STATs, and thus the activation of gene transcription and the following cytokine production and modulation of the immune response.

The original report in which it was described [23] provided evidence that tofacitinib inhibited JAK3 with an IC_{50} value of 1 nM while inhibiting JAK2 and JAK1 at higher IC_{50} values of 20 and 112 nM, respectively. Herein, we have reported an *in vitro* kinase assay to assess prodrug **2** ability to inhibit JAK1 and JAK3, and to compare it with tofacitinib's potency (Table 2, Fig. 3). Both prodrug **2** and tofacitinib were tested against the kinase of interest in 9-points concentrations, ranging from 1 nM to 10 μM. The resulted estimated IC_{50} values for tofacitinib (2.8 nM) correlated well with the reported value against JAK3, while a 30-fold discrepancy was observed for JAK1 (3.3 nM compared to 112 nM). This difference can arise from different experiment condition, especially for different ATP concentration used. Importantly, the difference from tofacitinib and prodrug **2** was remarkable with a calculated IC_{50} against JAK1 and JAK3 of 414 and 408 nM, respectively. This relatively strong effect of prodrug **2** against JAK1 and JAK3 could be explained by possible partial hydrolysis of the prodrug in the kinase assay buffer used or by unspecific interactions established by the aryl-boronic moiety. Despite the importance of tofacitinib pyrrolopyrimidine's hydrogen for establishing an hydrogen bond with E903 at the ATP binding site [24], other derivatives have shown their selectivity towards JAK3 through specific lipophilic interactions [8]. Nevertheless, the close to 200-fold difference indicates that prodrug **2** could have only minimal activity against the kinase of interest, mimicking tofacitinib pharmacodynamics only when freed from its aryl-boronic acid prodrug moiety.

2.5. Pharmacokinetics

The *in vivo* pharmacokinetic profiles for tofacitinib and prodrug **2** were compared. Tofacitinib citrate (80.8 mg/kg, equimolar to 50 mg/kg for tofacitinib free base) and equimolar doses of prodrug **2** were administered *i.p.* to DBA/1 mice [25]. Blood was collected from the treated mice at 0.25, 1, 7, and 24 h, and analyzed by LC-MS/MS. Even though tofacitinib showed an overall higher exposure level than prodrug **2**, good level of C_{max} (36.0 μM) and AUC_{calc} (1646 min*mg/L) were also found for prodrug **2** (Table 3). Tofacitinib's half-life agreed to literature's reported values (<1 h) [26,27] and prodrug **2** showed similar value. Calculated clearance (CL) was found similar between tofacitinib and prodrug **2** (low to moderate, 33.0 and 43.4 mL/min/kg, respectively). Remarkably, prodrug **2** showed stability in mouse plasma over 24 h, releasing less than 2% of tofacitinib over 24 h (data not shown).

Table 2
Estimated IC_{50} values (ATP concentrations: 45 μM for JAK1 and 10 μM for JAK3).

Compound	Kinase	IC_{50} (nM)
Tofaticinib Citrate	JAK1(h)	3.3 ± 1.1 (112) [23]
Tofaticinib Citrate	JAK3(h)	2.8 ± 1.1 (1) [23]
prodrug **2**	JAK1(h)	414.1 ± 1.1
prodrug **2**	JAK3(h)	408.8 ± 1.1

(h): human; measurements were obtained in duplicates; tofacitinib literature values are reported in brackets.

3. Conclusions

In this report, we have described the synthesis of new arylboronic acid-based hydrogen peroxide-sensitive tofacitinib prodrugs for putative RA inflammatory tissues site-selective delivery, with the aim of reducing side effects in tofacitinib therapy. Between the two prodrugs synthesized, prodrug **2** showed more favorable physicochemical properties and a slower activation profile under pathophysiological concentrations of H_2O_2. Prodrug **2** achieved complete conversion to the corresponding drug tofacitinib in the reasonable timeframe of 24 h (at a H_2O_2 concentration of 1 mM). Prodrug **2** activity against kinase of interest JAK1 and JAK3 was assessed using an *in vitro* kinase assay and proved to be around 150-fold lower than that of tofacitinib, indicating an attractive activity window, and validating the proof-of-concept prodrug strategy. Importantly, the pharmacokinetic data demonstrate that a single dose of prodrug **2** at 71.4 mg/kg achieved an exposure in plasma similar to tofacitinib citrate (80.8 mg/kg) for up to 7 h, exhibiting favorable ADME properties. These findings could open up future work on additional *in vivo* studies to establish drug/prodrug concentration in RA rodent models and, ultimately, antiarthritic efficacy to hopefully advance these promising prodrugs towards clinical evaluation.

4. Experimental

4.1. General

Commercially available reagents were used without further purification and all solvents were of HPLC quality. Reactions were monitored by thin layer chromatography (TLC) and/or reversed-phase ultra-performance liquid chromatography mass spectrometry (RP-UPLC-MS). Analytical TLC was conducted on Merck aluminum sheets covered with silica (C60) and visualized under UV-light. Analytical RP-UPLCMS (ESI) analysis was performed on a S2 Waters AQUITY RP-UPLC system equipped with a diode array detector using an Thermo Accucore C18 column (d 2.6 μm, 2.1 × 50 mm; column temp: 50 °C; flow: 1.0 mL/min). Eluents A (10 mM NH_4OAc in H_2O) and B (10 mM NH_4OAc in MeCN) were used in a linear gradient (5% B to 100% B) in 2.4 min and then held for 0.1 min at 100% B (total run time: 2.6 min). The LC system was coupled to a SQD mass spectrometer. All compounds were characterized by ^1H NMR, ^{13}C NMR, IR, HRMS (ESI), melting point, and specific rotation. Flash column chromatography was performed using Merck Geduran® Si 60 (40–63 μm) silica gel. Purification of reactions by preparative RP-HPLC was performed on a Waters Alliance reverse-phase HPLC system consisting of a Waters 2545 Binary Gradient Module equipped with either an xBridge BEH C18 OBD Prep Column (130 Å, 5 μm, 30 × 150 mm) or an xBridge Peptide BEH C18 OBD Prep Column (130 Å, 5 μm, 19 mm × 100 mm) both operating at 20 °C and a flow rate of 20 mL/min, a Waters. Photodiode Array Detector (detecting at 210–600 nm), a Waters UV Fraction Manager, and a Waters 2767 Sample Manager. Elution was carried out in a reversed-phase gradient fashion combining A1 (0.1% HCO_2H in milli-Q water) and B1 (0.1% HCO_2H in CH_3CN): 5% B to 70% B in 10 min, hold for 3.5 min, then 70% B to 100% B in 1.5 min, and hold 3 min. Total run time: 20 min. NMR data were acquired at 298 K using a Bruker Ascend spectrometer (operating at 400

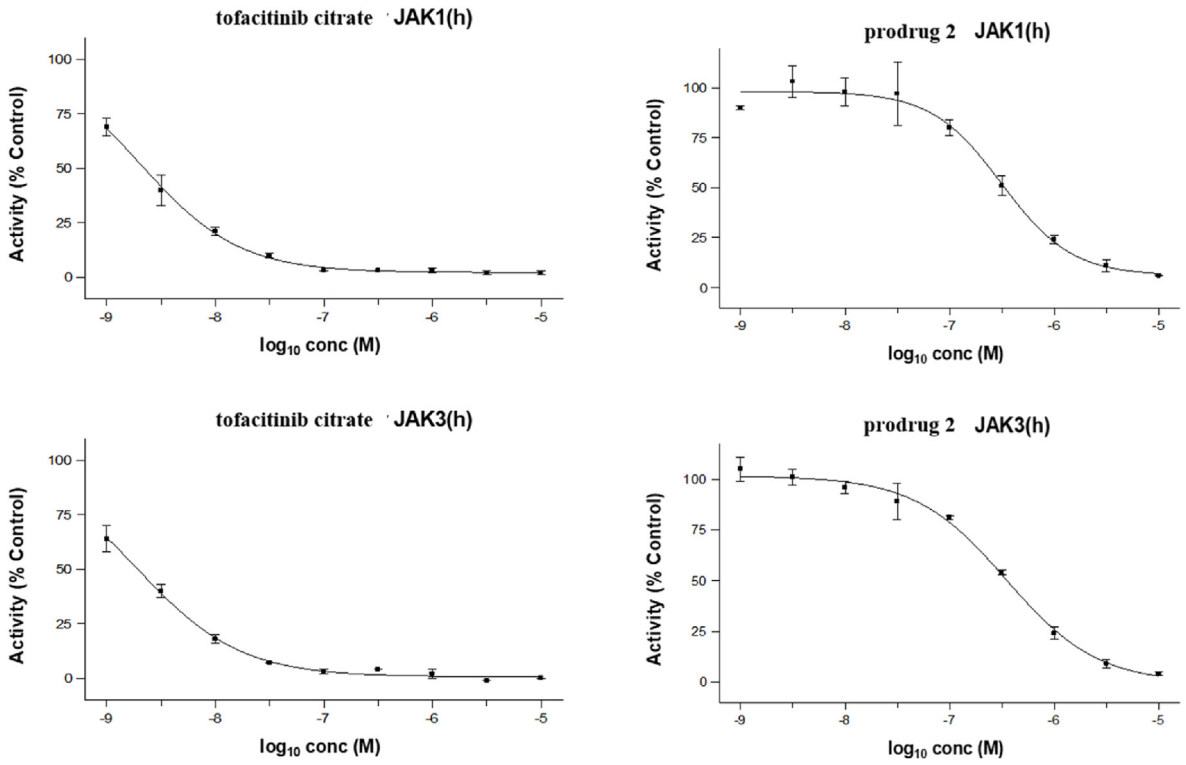

Fig. 3. IC_{50} dose-response curves of tofacitinib citrate against JAK1 and JAK3 (left), and of prodrug **2** (right).

Table 3
Pharmacokinetics parameters of **tofacitinib** and prodrug **2** in healthy DBA/1 mice.

	tofacitinib (citrate)	prodrug 2
Dose	80.8 mg/kg (*i.p.*)	71.4 mg/kg (*i.p.*)
C_{max}(obs)	33.4 mg/L (66.2 μM)	16.1 mg/L (36.0 μM)
T_{max}(obs)	15 min	15 min
$AUC_{0\text{-last}}$ (calc)	2445 min*mg/L	1646 min*mg/L
$t_{½}$ (calc)	<1 h	<1 h
CL (calc)	33.0 mL/min/kg	43.4 mL/min/kg

MHz for proton and 101 MHz for carbon). The chemical shifts (δ) are reported in parts per million (ppm) and the coupling constants (J) in Hz. For spectra recorded in DMSO-d_6, chemical shifts are reported relative to the signal for DMSO-d_6 (δ 2.50 ppm for ^{1}H NMR and δ 39.52 ppm for ^{13}C NMR). NMR data was analyzed using MestReNova (v11.0.0–17,609) by Mestrelab Research S.L. IR analysis was performed on a Bruker Alpha FT-IR spectrometer. Melting points were obtained using a Stuart SMP30 melting point apparatus and are uncorrected. Analytical LC-HRMS (ESI) analysis was performed on an Agilent 1100 RP-LC system equipped with a diode array detector using a Phenomenex Luna C18 column (d = 3 μm, 2.1 × 50 mm; column temp: 40 °C; flow: 0.4 mL/min). Eluents A (0.1% HCO_2H in H_2O) and B (0.1% HCO_2H in MeCN) were used in a linear gradient (20% B to 100% B) in a total run time of 15 min. The LC system was coupled to a Micromass LCT orthogonal time-of-flight mass spectrometer equipped with a Lock Mass probe operating in positive electrospray mode. Optical rotations were measured on a PerkinElmer Model 341 Polarimeter (cuvette 1.0 mL, 100 mm) using a sodium source lamp (589 nm, 20 °C).

4.2. Synthesis

4.2.1. 4-(4,4,5,5-Tetramethyl-1,3,2-dioxaborolan-2-yl)benzyl 4-(((3R,4R)-1-(2-cyanoacetyl)-4-methylpiperidin-3-yl)(methyl)amino)-7H-pyrrolo[2,3-d]pyrimidine-7-carboxylate (6)

To a suspension of tofacitinib citrate (1.78 mmol, 1 equiv.) in CH_2Cl_2 (17 mL) was added DIPEA (10.68 mmol, 6 equiv.). After 30 minutes of stirring, 4-(4,4,5,5-tetramethyl-1,3,2-dioxaborolan-2-yl)benzyl carbonochloridate (**5**) (2.14 mmol, 1.2 equiv.) in CH_2Cl_2 (6 mL) was added and the reaction cooled to 0 °C. After stirring for 4 h at 0 °C, H_2O was added to quench excess reagent and the crude mixture was extracted with CH_2Cl_2. The organic layer was dried over Na_2SO_4, filtered, and dried *in vacuo*. The residue was purified by flash chromatography (heptane:EtOAc, 20:80 -> 0:100) to afford the title compound as a white solid (208 mg, 20%). **^{1}H-NMR** (400 MHz, DMSO-d_6): δ 8.34–8.32 (m, 1H), 7.71 (d, J = 7.7 Hz, 2H), 7.57–7.57 (m, 3H), 6.89–6.87 (m, 1H), 5.50 (s, 2H), 4.85 (bs, 1H), 4.17–3.91 (m, 3H), 3.84–3.63 (m, 2H), 3.41–3.40 (m, 1H), 3.26 (s, 3H), 2.41–2.33 (m, 1H), 1.87–1.67 (m, 1H), 1.61–1.53 (m, 1H), 1.29 (s, 12H), 1.00 (d, J = 7.1 Hz, 3H). **^{13}C-NMR** (101 MHz, DMSO-d_6): δ 161.60, 161.49, 157.01, 152.53, 152.14, 148.99, 138.70, 134.59, 127.05, 121.70, 116.21, 106.63, 104.51, 83.71, 68.21, 53.08, 42.40, 41.59, 34.43, 30.89, 30.69, 24.92, 24.65, 13.70. **HRMS (ESI)** *m/z*: calcd for $C_{30}H_{37}BN_6O_5$ $[M+H]^+$ 573.2918, found 573.2913. **IR** (neat, cm^{-1}): 2976.33, 2930.71, 1758.90, 1739.88, 1658.99, 1567.48, 1532.84, 1357.51, 1294.93, 1271.47, 1166.11, 1140.81, 1087.16, 1013.54, 856.84, 720.03, 657.11. **m.p.**: 123–125 °C. $[\alpha]_D^{20}$ + 13.1° (*c* 0.38, $CHCl_3$).

4.2.2. (4-(((4-(((3R,4R)-1-(2-Cyanoacetyl)-4-methylpiperidin-3-yl)(methyl)amino)-7H-pyrrolo[2,3-d]pyrimidine-7-carbonyl)oxy)methyl)phenyl)boronic acid (1)

To a solution of pinacol precursor **6** (0.20 mmol, 1 equiv.) in acetone (2.5 mL), a 500 mM aq. solution of NH_4OAc in H_2O (1.20 mmol, 6 equiv.), and $NaIO_4$ (1.20 mmol, 6 equiv.) were added. After 2 hours stirring at room temperature, the precipitate was filtered off and the mixture evaporated *in vacuo*. The residue was purified by flash chromatography (CH_2Cl_2:2-propanol, 90:10 -> 80:20) to afford the title compound as a white solid (70 mg, 70%). **^{1}H-NMR** (400 MHz, DMSO-d_6): δ 8.33–8.32 (m, 1H), 8.08 (s, 2H), 7.82 (d, $J = 7.9$ Hz, 2H), 7.58 (d, $J = 4.2$ Hz, 1H), 7.50 (d, $J = 7.9$ Hz, 2H), 6.89–6.86 (m, 1H), 5.48 (s, 2H), 4.85 (bs, 1H), 4.17–3.91 (m, 3H), 3.84–3.63 (m, 2H), 3.46–3.40 (m, 1H), 3.26 (s, 3H), 2.41–2.34 (m, 1H), 1.86–1.68 (m, 1H), 1.60–1.53 (m, 1H), 1.04–0.99 (m, 3H). **^{13}C-NMR** (101 MHz, DMSO-d_6): δ 161.61, 161.50, 157.02, 152.51, 152.15, 149.01, 137.08, 134.27, 126.74, 121.76, 116.23, 106.62, 104.52, 68.43, 53.10, 42.41, 41.60, 34.43, 30.91, 30.66, 24.93, 13.71. **HRMS (ESI)** *m/z*: calcd for $C_{24}H_{27}BN_6O_5$ $[M+H]^+$ 491.2136, found 491,2133. **IR** (neat, cm^{-1}): 2966.60, 2927.43, 1754.55, 1650.32, 1569.49, 1533.98, 1492.50, 1454.01, 1433.69, 1411.70, 1379.66, 1332.74, 1294.77, 1276.06, 1166.98, 1125.46, 1013.60, 978.6, 950.16, 719.37. **m.p.**: 190 °C (decomp). $[\alpha]_D^{20}$ + 8.6° (*c* 0.49, DMSO).

4.2.3. (4-((4-(((3R,4R)-1-(2-Cyanoacetyl)-4-methylpiperidin-3-yl)(methyl)amino)-7H-pyrrolo[2,3-d]pyrimidin-7-yl)methyl)phenyl)boronic acid (2)

To a solution of tofacitinib free base (1.13 mmol, 1 equiv.) in DMF (4.5 mL), DIPEA (2.26 mmol, 2 equiv.) and (4-(bromomethyl)phenyl) boronic acid **8** (1.36 mmol, 1.2 equiv.) were added. After 2 h stirring at 55 °C, the mixture was evaporated *in vacuo* and the mixture purified with reverse phase preparative HPLC to afford the title compound as a white solid (138 mg, 27%). **^{1}H-NMR** (400 MHz, DMSO-d_6): δ 8.62–8.57 (m, 1H), 8.22 (s, 2H), 7.72 (d, $J = 7.7$ Hz, 2H), 7.38–7.27 (m, 3H), 6.71 (s, 1H), 5.56 (s, 2H), 4.95 (bs, 1H), 4.17–3.95 (m, 3H), 3.82–3.65 (m, 2H), 3.40–3.35 (m, 4H), 2.39 (s, 1H), 1.83–1.71 (m, 1H), 1.61–1.58 (m, 1H), 1.02–1.01 (m, 3H). **^{13}C-NMR** (101 MHz, DMSO-d_6): δ 163.81, 161.58, 155.96, 142.44, 137.55, 134.31, 133.58, 126.85, 126.76, 116.22, 104.31, 104.10, 54.90, 51.57, 42.38, 41.48, 34.84, 31.21, 30.84, 24.95, 13.65. **HRMS** (ESI) *m/z*: calcd for $C_{23}H_{27}BN_6O_3$ $[M+H]^+$ 447.2238, found 447.2219. **IR** (neat, cm^{-1}): 3306.43, 3080.63, 3051.90, 2930.64, 2798.93, 1650.93, 1615.02, 1575.50, 1540.22, 1514.45, 1454.02, 1409.77, 1372.31, 1337.62, 1250.77, 1218.64, 1182.95, 1122.99, 1016.93, 732.45. **m.p.**: 219 °C (decomp.). $[\alpha]_D^{20}$ + 5.8° (*c* 0.36, DMSO).

4.2.4. Benzyl 4-(((3R,4R)-1-(2-cyanoacetyl)-4-methylpiperidin-3-yl)(methyl)amino)-7H-pyrrolo[2,3-d]pyrimidine-7-carboxylate (3)

To a suspension of tofacitinib citrate (0.59 mmol, 1 equiv.) in CH_2Cl_2 (10 mL) was added DIPEA (3.57 mmol, 6 equiv.). After 15 minutes of stirring, CbzCl **7** (0.71 mmol, 1.2 equiv.) in CH_2Cl_2 (3 mL) was added and the reaction cooled to 0 °C. After stirring for 1 h at 0 °C, the reaction was left stirring overnight at room temperature. H_2O was then added to quench excess reagent and the crude mixture was extracted with CH_2Cl_2. The organic layer was dried over Na_2SO_4, filtered, and dried *in vacuo*. The residue was purified by flash chromatography (heptane:EtOAc, 20:80 -> 0:100) to afford the title compound as a pink solid (144 mg, 54%). **^{1}H-NMR** (400 MHz, DMSO-d_6): δ 8.33–8.32 (m, 1H), 7.57–7.54 (m, 3H), 7.44–7.34 (m, 3H), 6.88–6.84 (m, 1H), 5.48 (s, 2H), 4.84 (bs, 1H), 4.19–3.91 (m, 3H), 3.85–3.62 (m, 2H), 3.42–3.40 (m, 1H), 3.26 (s, 3H), 2.40–2.33 (m, 1H), 1.85–1.66 (m, 1H), 1.60–1.56 (m, 1H), 1.00 (d, $J =$ 7.1 Hz, 3H). **^{13}C-NMR** (101 MHz, DMSO-d_6): δ 161.61, 161.49, 157.01, 152.51, 152.14, 148.99, 135.40, 128.53, 128.28, 127.92, 121.73, 116.22, 106.56, 104.51, 68.43, 53.07, 42.41, 41.60, 34.43, 30.89, 30.66, 30.00, 24.92, 13.71. **HRMS** (ESI) *m/z*: calcd for $C_{24}H_{26}N_6O_3$ $[M+H]^+$ 447.2066, found 447.2057. **IR** (neat, cm^{-1}): 2933.93, 1732.86, 1653.01, 1566.97, 1532.01, 1453.83, 1294.91, 1166.28, 1014.14, 719.82. **m.p.**: 75–76 °C. $[\alpha]_D^{20}$ + 19.5° (*c* 0.37, $CHCl_3$).

4.3. Chemical stability and PAMPA assay

4.3.1. Activation with hydrogen peroxide (H_2O_2)

Prodrug 1: 50 μL of a 1 mM solution of prodrug 1 in DMSO was added to PBS (375 μL) together with 50 μL of a 1 mM DMSO solution of diclofenac. For activation, 25 μL of 20 mM or 5 mM H_2O_2 solution in PBS were added. The solution was then mixed and placed in an Eppendorf Thermomixer (1000 rpm, 37 °C). Aliquots of 50 μL were taken after 0 min, 15 min, 30 min, 1 h, 2 h, 4 h and 24 h. Analysis was performed as detailed in the analysis section below.

Prodrug 2: 50 μL of a 20 mM solution of prodrug 2 in DMSO was diluted with 425 μL of water and 25 μL of 20 mM H_2O_2 solution was added. 200 μL of the solution was transferred to a vial and immediately to the UPHLC-MS instrument for analysis. Analysis by UHPLC-MS/MS was performed at 0 min, 15 min, 30 min, 1 h, 2 h, 4, 8 h, and 24 h. The data was normalized to the 0 minutes data for prodrug 2 and to the 24 h data for tofaticinib.

4.3.2. Stability in PBS

Prodrug (2 μL, 10 mM in DMSO) was added to a solution of pre-warmed PBS (1998 μL) to obtain a final prodrug concentration of 10 μM (0.1% DMSO). 500 μL of the mixture was then placed in an Eppendorf Thermomixer C (1.5 mL, 1000 rpm). Aliquots of 50 μL were taken after 0, 2, 4, 6 and 24 h and quenched with 50 μL of ice-cold MeOH containing an internal standard (diclofenac 10 μM, 0.1% DMSO). Analysis was performed as detailed in the analysis section below.

4.3.3. Stability in simulated gastric fluid (SGF) [20]

Sodium chloride (0.20 g), concentrated HCl (0.70 mL), and pepsin (Sigma, P-7000, 0.32 g) were added to deionized water (99.30 mL) to obtain a simulated gastric fluid (SGF) solution with a final volume of 100 mL. A solution of prodrug (10 μL, 10 mM in DMSO) was added to a solution of SGF (990 μL) and the mixture was incubated at 37 °C in an Eppendorf Thermomixer C (1.5 mL, 1000 rpm). Aliquots of 90 μL were taken after 0, 1, 2, 4, and 24 h. To the aliquots was added 10 μL of diclofenac (1 mM in DMSO) as an internal standard. Analysis was performed as detailed in the analysis section below.

4.3.4. Stability in simulated intestinal fluid (SIF) [20]

Monobasic potassium phosphate (KH_2PO_4, 0.68 g), sodium hydroxide (38 mL, 0.1 M, aq.), and pancreatin (Sigma, P-1625, 1.0 g) were added to deionized water (62 mL) to obtain the simulated

intestinal fluid (SIF) with a final volume of 100 mL. Using a pH-meter the pH of the solution was adjusted to 7.5 by the addition of sodium hydroxide (1 M, aq.). A solution of prodrug (10 μL, 10 mM in DMSO) was added to a solution of SIF (990 μL) and the mixture was incubated at 37 °C in an Eppendorf Thermomixer C (1.5 mL, 1000 rpm). Aliquots of 180 μL were taken after 0, 1, 2, 4, and 24 h. The aliquots were transferred to an Eppendorf and centrifuged. Samples of 90 μL of the supernatant was taken and diclofenac (10 μL, 1 mM in DMSO) as an internal standard. Analysis was performed as detailed in the analysis section below.

4.3.5. Analysis

Samples were collected at the desired time points and then analyzed with RP-UPLC-MS (λ = 306 nm). The % remaining compound was calculated using diclofenac as an internal standard and using the following equations. All experiments were done in at least three replicates.

$$\text{ratio} = \frac{\text{AUC prodrug}}{\text{AUC diclofenac}}$$

$$\%\text{remaining} = \frac{\text{ratio at time point}}{\text{ratio at t} = 0} * 100$$

4.4. PAMPA assay

The PAMPA assay was performed using Corning® BioCoat™ Pre-coated PAMPA Plate System (Product number: 353,015) following a previously reported procedure [28,29]. Compound solutions were prepared by diluting 20 μL of 20 mM stock solutions (DMSO) with 1980 μL of PBS. Caffeine was used as positive control. To the donor well was added 300 μL/well of the 200 μM test compound solution. To the acceptor well was added 200 μL/well of PBS. The acceptor plate was then slowly placed on top of the donor plate and incubated at room temperature for 5 h with no agitation. Samples of 150 μL from both the donor and the corresponding acceptor well were analyzed using RP-UPLC-MS (λ = 306 nm) and concentration extrapolated with previously obtained calibration curves. The results were calculated as the average of at least three replicates. The permeability coefficients (Pe, cm/s) of the examined compounds were calculated using the following formula provided by the PAMPA Plate System manufacturer [30].

$$Pe = \left[-\ln\left(1 - C_A / C_{eq}\right)\right] / \left[A * (1 / V_D + 1 / V_A) * t\right]$$

where C_A is the compound concentration in the acceptor well after 5 hours; C_D is the compound concentration in the donor well after 5 hours; V_A is the volume in acceptor well (200 μL); V_D is the volume in the donor well (300 μL), t is the incubation time (s); and A is the filter area (0.3 cm^2). C_{eq} is calculated using the equation below:

$$C_{eq} = \left[(C_D * V_D) + (C_A * V_A)\right] / (V_D + V_A)$$

4.5. In vitro kinase assay

Prodrug **2** and tofacitinb were assessed for binding at JAK1 and JAK3 protein kinases using a direct filter-binding radiometric kinase activity assay (KinaseProfiler™ - Eurofins). 9-point IC_{50} curves were provided ranging from 1 nM to 10 μM and using ATP concentrations of 45 μM for JAK1 and 10 μM for JAK3. IC_{50} were calculated using GraphPrism and log(inhibitor) vs. normalized response as non linear regression (curve fit).

4.6. In vivo pharmacokinetic

4.6.1. Mice

Six-week-old, female DBA/1JRj mice were purchased (Janvier, Le Genest-Saint-Isle, France) and housed in groups of 8 mice in individually ventilated cages under standardized lighting conditions (12 h light period) and fed pathogen-free food and water ad libitum. Mice were acclimatized for one week prior to the experiment. The animal experiment had been approved by The Animal Experiments Inspectorate in Denmark under the license number 2016-15-0201-00920, approved on 5 July 2016.

4.7. Single dose tofacitinib/prodrug 2 intervention and sampling

Mice were randomly divided into two groups (n = 8/group): group I (**tofacitinib**, 80.8 mg/kg, *i.p.*) and group II (prodrug **2**, 71.4 mg/kg, *i.p.*). Mice were treated with a single dose of **tofacitinib**/prodrug **2** and blood was collected from vena sublingualis at 0.25, 1, 7, and 24 h after administration. Both treatments were equimolar to 50 mg/kg for tofacitinib free base. The samples were stored at −80 °C until analysis by LC-MS/MS.

4.7.1. Sample preparation for UHPLC-MS/MS

40 μL of whole blood was transferred to an Eppendorf tube and 160 μL of ultrapure water was added followed by 200 μL of methanol and 600 μL of acetonitrile. The samples were mixed (10 s, 1500 rpm) using a benchtop vortex mixer and macromolecules allowed to precipitate for 10 minutes and room temperature. The precipitate was pelleted by centrifugation (10,000 g, 10 minutes, 4 °C) and 500 μL of supernatant transferred to a clean eppendorf tube and concentrated using a SpeedVac. The samples were redissolved in 100 μL of ultrapure water and analyzed using UHPLC-MS/MS. This method was adapted from work by Sørensen, L. K. and co-workers [31].

4.7.2. UHPLC-MS/MS analysis

The samples were analyzed using a Shimadzu LCMS-8045 LCMS equipped with a Phenomex C18 column (100 × 2.1 mm, 2.6 μm) kept at 40 °C. Mobile phase A was water with 0.1% formic acid and mobile phase B was acetonitrile with 0.1% formic acid. Flow rate: 0.5 mL/min. Gradient: Isocratic 10% B minute 0–0.5, linear from 10% to 60% B minute 0.5–3, linear from 60% to 100% B minute 3–3.50, isocratic 100% B minute 3.50–4, linear from 100% B to 10% B minute 4–4.50, isocratic 10% B minute 4.50–6. Injection: 5 μL. For analysis of blood samples an external standard series was used to obtain semi-quantitative results. For MS-specifications refer to table below.

Quantification	Target	Mode	Precursor *m/z*	Product *m/z*	rt	Q1 Bias (V)	Q3 Bias (V)	CE (V)
$[M+H]^+$	Tofaticinib	+	313,20	149,25	1.742	−21	−28	−30
$[M+H]^+$	Prodrug 2	+	447,20	283,20	2.670	−16	−14	−27
Qualifying								
$[M+H]^+$	Tofaticinib	+	313,20	173,20	1.742	−21	−17	−37
$[M+H]^+$	Tofaticinib	+	313,20	98,20	1.742	−21	−18	−32
$[M+H]^+$	Prodrug 2	+	447,20	135,15	2.670	−16	−24	−33
$[M+H]^+$	Prodrug 2	+	447,20	117,10	2.670	−22	−21	−55

5. Chemical compounds studied in this article

Tofacitinib (PubChem CID: 9926791).

Acknowledgments

We are grateful for financial support from the Independent Research Fund Denmark (grant no. 7017–00026) and the Technical University of Denmark (PoC funding). Graphical abstract image was created with BioRender.com.

Appendix A. Supplementary data

Supplementary data to this article can be found online at https://doi.org/10.1016/j.ejmcr.2021.100019.

References

[1] P. Cohen, D. Cross, P.A. Jänne, Kinase drug discovery 20 years after imatinib: progress and future directions, Nat. Rev. Drug Discov. (2021).
[2] P.O. Guimarães, D. Quirk, R.H. Furtado, L.N. Maia, J.F. Saraiva, M.O. Antunes, R. Kalil Filho, V.M. Junior, A.M. Soeiro, A.P. Tognon, V.C. Veiga, P.A. Martins, D.D.F. Moia, B.S. Sampaio, S.R.L. Assis, R.V.P. Soares, L.P.A. Piano, K. Castilho, R.G.R.A.P. Momesso, F. Monfardini, H.P. Guimarães, D. Ponce de Leon, M. Dulcine, M.R.T. Pinheiro, L.M. Gunay, J.J. Deuring, L.V. Rizzo, T. Koncz, O. Berwanger, Tofacitinib in patients hospitalized with covid-19 pneumonia, N. Engl. J. Med. (2021).
[3] G.E. Fragoulis, I.B. McInnes, S. Siebert, JAK-inhibitors. New players in the field of immune-mediated diseases, beyond rheumatoid arthritis, Rheumatology 58 (Suppl 1) (2019) i43–i54.
[4] R. Harrington, S.A. Al Nokhatha, R. Conway, JAK inhibitors in rheumatoid arthritis: an evidence-based review on the emerging clinical data, J. Inflamm. Res. 13 (2020) 519–531.
[5] J. Angelini, R. Talotta, R. Roncato, G. Fornasier, G. Barbiero, L. Dal Cin, S. Brancati, F. Scaglione, JAK-inhibitors for the treatment of rheumatoid arthritis: a focus on the present and an outlook on the future, Biomolecules 10 (7) (2020).
[6] J.A. Hodge, T.T. Kawabata, S. Krishnaswami, J.D. Clark, J.B. Telliez, M.E. Dowty, S. Menon, M. Lamba, S. Zwillich, The mechanism of action of tofacitinib - an oral Janus kinase inhibitor for the treatment of rheumatoid arthritis, Clin. Exp. Rheumatol. 34 (2) (2016) 318–328.
[7] R. Fleischmann, A review of tofacitinib efficacy in rheumatoid arthritis patients who have had an inadequate response or intolerance to methotrexate, Expet Opin. Pharmacother. 18 (14) (2017) 1525–1533.
[8] J.D. Clark, M.E. Flanagan, J.B. Telliez, Discovery and development of Janus kinase (JAK) inhibitors for inflammatory diseases, J. Med. Chem. 57 (12) (2014) 5023–5038.
[9] R. The Lancet, JAK inhibitors: fate in doubt for rheumatoid arthritis? The Lancet Rheumatology 3 (3) (2021) e161.
[10] J.J. O'Shea, M. Gadina, Selective Janus kinase inhibitors come of age, Nat. Rev. Rheumatol. 15 (2) (2019) 74–75.
[11] Y. Tanaka, Recent progress and perspective in JAK inhibitors for rheumatoid arthritis: from bench to bedside, J. Biochem. 158 (3) (2015) 173–179.
[12] J. Peiró Cadahía, V. Previtali, N.S. Troelsen, M.H. Clausen, Prodrug strategies for targeted therapy triggered by reactive oxygen species, Med. Chem. Commun. 10 (9) (2019) 1531–1549.
[13] H. Maslah, C. Skarbek, S. Pethe, R. Labruère, Anticancer boron-containing prodrugs responsive to oxidative stress from the tumor microenvironment, Eur. J. Med. Chem. 207 (2020) 112670.
[14] P. Wang, Q. Gong, J. Hu, X. Li, X. Zhang, Reactive oxygen species (ROS)-Responsive prodrugs, probes, and theranostic prodrugs: applications in the ROS-related diseases, J. Med. Chem. 64 (1) (2021) 298–325.
[15] K. Matsushita, T. Okuda, S. Mori, M. Konno, H. Eguchi, A. Asai, J. Koseki, Y. Iwagami, D. Yamada, H. Akita, T. Asaoka, T. Noda, K. Kawamoto, K. Gotoh, S. Kobayashi, Y. Kasahara, K. Morihiro, T. Satoh, Y. Doki, M. Mori, H. Ishii, S. Obika, A hydrogen peroxide activatable gemcitabine prodrug for the selective treatment of pancreatic ductal adenocarcinoma, ChemMedChem 14 (15) (2019) 1384–1391.
[16] M. Lu, X. Zhang, J. Zhao, Q. You, Z. Jiang, A hydrogen peroxide responsive prodrug of Keap1-Nrf2 inhibitor for improving oral absorption and selective activation in inflammatory conditions, Redox Biol 34 (2020) 101565.
[17] J.E. Palmer, B.M. Brietske, T.C. Bate, E.A. Blackwood, M. Garg, C.C. Glembotski, C.B. Cooley, Reactive oxygen species (ROS)-Activatable prodrug for selective activation of ATF6 after ischemia/reperfusion injury, ACS Med. Chem. Lett. 11 (3) (2020) 292–297.
[18] Q. Bao, L. Zhang, N. Wang, B. Gabet, W. Yang, X. Gao, Q. You, Z. Jiang, Hydrogen peroxide inducible JAK3 covalent inhibitor: prodrug for the treatment of RA with enhanced safety profile, ACS Med. Chem. Lett. 11 (11) (2020) 2182–2189.
[19] X. Wei, J. Wu, G. Zhao, J. Galdamez, S.M. Lele, X. Wang, Y. Liu, D.M. Soni, P.E. Purdue, T.R. Mikuls, S.R. Goldring, D. Wang, Development of a Janus kinase inhibitor prodrug for the treatment of rheumatoid arthritis, Mol. Pharm. 15 (8) (2018) 3456–3467.
[20] J. Peiró Cadahía, J. Bondebjerg, C.A. Hansen, V. Previtali, A.E. Hansen, T.L. Andresen, M.H. Clausen, Synthesis and evaluation of hydrogen peroxide sensitive prodrugs of methotrexate and aminopterin for the treatment of rheumatoid arthritis, J. Med. Chem. 61 (8) (2018) 3503–3515.
[21] N.S. Andersen, J. Peiró Cadahía, V. Previtali, J. Bondebjerg, C.A. Hansen, A.E. Hansen, T.L. Andresen, M.H. Clausen, Methotrexate prodrugs sensitive to reactive oxygen species for the improved treatment of rheumatoid arthritis, Eur. J. Med. Chem. 156 (2018) 738–746.
[22] A. Daina, O. Michielin, V. Zoete, SwissADME: a free web tool to evaluate pharmacokinetics, drug-likeness and medicinal chemistry friendliness of small molecules, Sci. Rep. 7 (1) (2017) 42717.
[23] P.S. Changelian, M.E. Flanagan, D.J. Ball, C.R. Kent, K.S. Magnuson, W.H. Martin, B.J. Rizzuti, P.S. Sawyer, B.D. Perry, W.H. Brissette, S.P. McCurdy, E.M. Kudlacz, M.J. Conklyn, E.A. Elliott, E.R. Koslov, M.B. Fisher, T.J. Strelevitz, K. Yoon, D.A. Whipple, J. Sun, M.J. Munchhof, J.L. Doty, J.M. Casavant, T.A. Blumenkopf, M. Hines, M.F. Brown, B.M. Lillie, C. Subramanyam, C. Shang-Poa, A.J. Milici, G.E. Beckius, J.D. Moyer, C. Su, T.G. Woodworth, A.S. Gaweco, C.R. Beals, B.H. Littman, D.A. Fisher, J.F. Smith, P. Zagouras, H.A. Magna, M.J. Saltarelli, K.S. Johnson, L.F. Nelms, S.G. Des Etages, L.S. Hayes, T.T. Kawabata, D. Finco-Kent, D.L. Baker, M. Larson, M.S. Si, R. Paniagua, J. Higgins, B. Holm, B. Reitz, Y.J. Zhou, R.E. Morris, J.J. O'Shea, D.C. Borie, Prevention of organ allograft rejection by a specific Janus kinase 3 inhibitor, Science 302 (5646) (2003) 875–878.
[24] J.-k. Jiang, K. Ghoreschi, F. Deflorian, Z. Chen, M. Perreira, M. Pesu, J. Smith, D.-T. Nguyen, E.H. Liu, W. Leister, S. Costanzi, J.J. O'Shea, C.J. Thomas, Examining the chirality, conformation and selective kinase inhibition of 3-((3R,4R)-4-methyl-3-(methyl(7H-pyrrolo[2,3-d]pyrimidin-4-yl)amino)piperidin-1-yl)-3-oxopropanenitrile (CP-690,550), J. Med. Chem. 51 (24) (2008) 8012–8018.
[25] M.E. Dowty, M.I. Jesson, S. Ghosh, J. Lee, D.M. Meyer, S. Krishnaswami, N. Kishore, Preclinical to clinical translation of tofacitinib, a Janus kinase inhibitor, in rheumatoid arthritis, J. Pharmacol. Exp. Therapeut. 348 (1) (2014) 165–173.
[26] A. Dixit, S.R. Mallurwar, S.P. Sulochana, M. Zainuddin, R. Mullangi, Determination of tofacitinib in mice whole blood on dried blood spots using LC-ESI-MS/MS: application to pharmacokinetic study in mice, Drug Res. 69 (6) (2019) 330–336.
[27] J.S. Lee, H.S. Kim, Y.S. Jung, H.G. Choi, S.H. Kim, Pharmacokinetic drug interaction between tofacitinib and voriconazole in rats, Pharmaceutics 13 (5) (2021).
[28] V. Previtali, K. Petrovic, J. Peiró Cadahía, N.S. Troelsen, M.H. Clausen, Auxiliary in vitro and in vivo biological evaluation of hydrogen peroxide sensitive prodrugs of methotrexate and aminopterin for the treatment of rheumatoid arthritis, Bioorg. Med. Chem. Lett 28 (2) (2020) 115247.
[29] G. Latacz, A. Lubelska, M. Jastrzębska-Więsek, A. Partyka, A. Sobiło, A. Olejarz, K. Kucwaj-Brysz, G. Satała, A.J. Bojarski, A. Wesołowska, K. Kieć-Kononowicz, J. Handzlik, In the search for a lead structure among series of potent and selective hydantoin 5-HT7R agents: the drug-likeness in vitro study, Chem. Biol. Drug Des. 90 (6) (2017) 1295–1306.
[30] Corning® BioCoat™ Pre-coated PAMPA Plate System.
[31] L.K. Sørensen, N.F. Rittig, E.F. Holmquist, K.A. Jørgensen, J.O.L. Jørgensen, N. Møller, M. Johannsen, Simultaneous determination of β-hydroxybutyrate and β-hydroxy-β-methylbutyrate in human whole blood using hydrophilic interaction liquid chromatography electrospray tandem mass spectrometry, Clin. Biochem. 46 (18) (2013) 1877–1883.